Available online: http://journal.uir.ac.id/index.php/JEEE/index

Journal of Earth Energy Engineering

Publisher: Universitas Islam Riau (UIR) Press

4-dimensional seismic interpretation to monitor CO2 injection in carbon capture & storage project of Sleipner field, North Sea, Norway using inversion method

Brimas Aptanindia Pangestu[1*], Muhammad Husni Mubarak Lubis[1]
[1]Faculty of Exploration and Production Technology, Pertamina University, Jl. Teuku Nyak Arief, Jakarta, West Java, Indonesia - 12220
*Corresponding Author: brimasaptanindiapangestu@gmail.com

Article History:

Received: May 20, 2023
Receive in Revised Form: May 31, 2023
Accepted: June 10, 2023

Keywords:

Carbon capture and storage, saline aquifer, 4-dimensional inversion, repeatability, normalized root mean square.

Abstract

Sleipner is the world's first commercial Carbon Capture and Storage (CCS) project, located off the coast of Norway, with the goal of reducing carbon emissions by capturing CO2 and storing it in a utsira saline aquifer sandstone reservoir capable of storing up to 600 billion tonnes of CO2. The CO2 injection in these projects increases year after year, so the CO2 development must be monitored to see the distribution pattern and its implications for the reservoir zone. The purpose of this research is to calculate and model the CO2 distribution resulting from acoustic impedance inversion using 4-dimensional inversion, to calculate the repeatability from seismic data between baseline and monitor using the Normalized Root Mean Square attribute. In the processing, baseline and monitor data must be matched in the overburden zone using a cross-equalization process so that the inversion process. The results revealed a correlation between the two seismic data sets (baseline and monitor) with the classification of Reasonable Repeatability, and CO2 distribution in a securely stored reservoir that spreads laterally and does not leak.

INTRODUCTION

Carbon Capture and Storage (CCS) technology is one solution that can be implemented quickly and on a large scale. This technology is an activity that involves capturing CO_2 (capture) from CO_2 emission sources such as natural gas processing facilities and power plants (source) and transporting it to CO_2 storage locations in geological storage such as empty oil wells or gas reservoirs, saline aquifer beds, coal seams, and other similar rock formations.

The goal of this research is to calculate and model the CO_2 distribution as a result of acoustic impedance inversion in 4D. Then, using the Normalized Root Mean Square attribute, compute the repeatability value of seismic data between the baseline and the monitor.

This study was conducted in the Sleipner field in Norway's North Sea (Figure 1). The Sleipner Field is a gas-producing field located 3400-3600 meters below the earth's surface in the Heimdal formation. This field's gas production also contains about 9% CO_2. In order to meet the requirements or specifications for energy sales, the CO_2 content emitted must be reduced to 2.5 percent. With these constraints, the field operator considers injecting CO_2 into the earth to reduce CO_2 emissions (Chadwick et al, 2005).

The utsira reservoir serves as a storage facility for CO_2 injection in the Sleipner gas field, with approximately one million tons of CO_2 injected into it each year. The Utsira FM reservoir is a saline aquifer sandstone type that is suitable for CO_2 storage due to its high porosity and permeability. This utsira formation is approximately 800 to 1000 meters deep and 200 to 300 meters thick in the earth (Figure 2). The utsira sandstone reservoir formed during the Miocene to Pliocene epochs and is axially located in a thick post-rift succession to the north of the North Sea Basin (Chadwick, 2010).

DOI: 10.25299/jeee.2023.14098
eISSN: 2540-9352 pISSN: 2301-8097

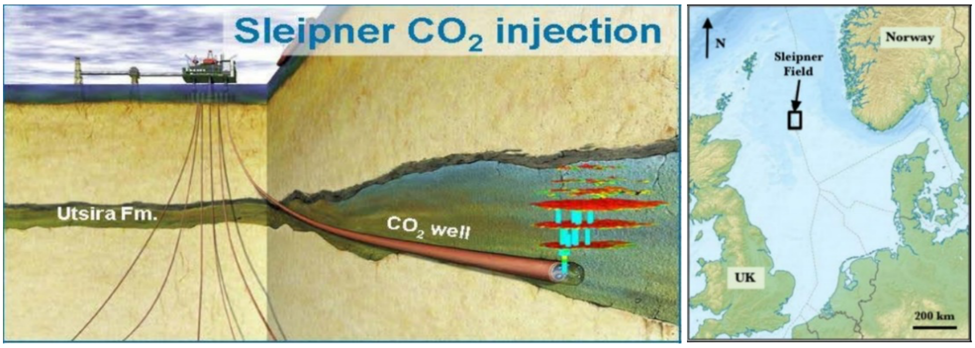

Figure 1. Location of Sleipner field (Solheim, 2021) and illustration of Sleipner field CO_2 injection (Chadwick et al., 2010).

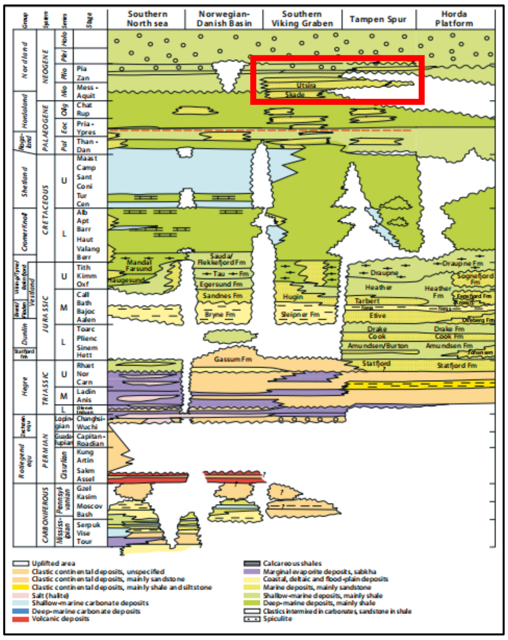

Figure 2. Litostratigraphic chart in the North Sea (Norwegian Petroleum Directorate, 2011).

MATERIALS AND METHODS

The data used is open-source data made available under the Sleipner CO_2 Dataset License. Full stack 3D seismic data from 1994 and 2004 (Figure 3), reprocessed in 2007, as well as injection and exploration well data from the Equinor company, were used. The seismic data used is 3D seismic data from 1994 as baseline data and 2004 as monitor data that was reprocessed in 2007.

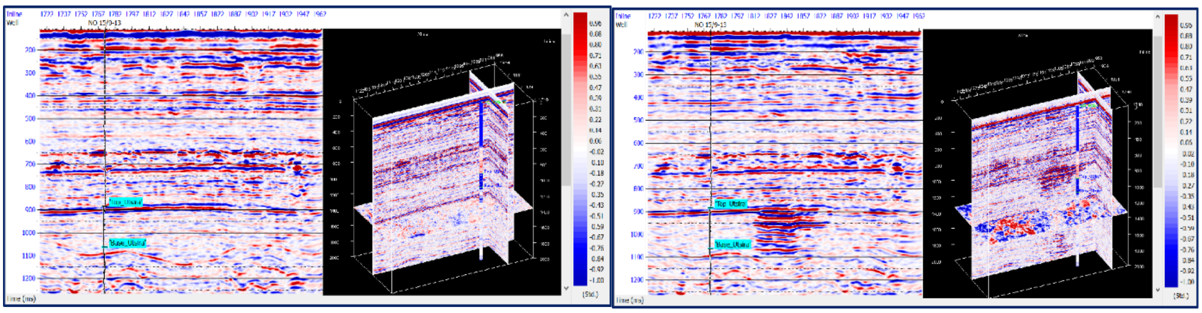

Figure 3. 1994 3D seismic data Baseline (left), 2004 3D seismic data Monitor (right).

In this study, the well data obtained from open source data are injection and exploration wells, but only onwell is used in the processing of this research, namely exploration wells, because the injection wells are outside the seismic survey location and cannot be processed later, either in the well tie process or in the inversion process, and the availability of incomplete log data on injection wells is not used as a reference for these wells. A seismic survey map and trajectory wells are shown below (Figure 4).

Journal of Earth Energy Engineering
Vol. 12 No. 2s 2023: IC-UPERTAIN 2022, pp 53-66

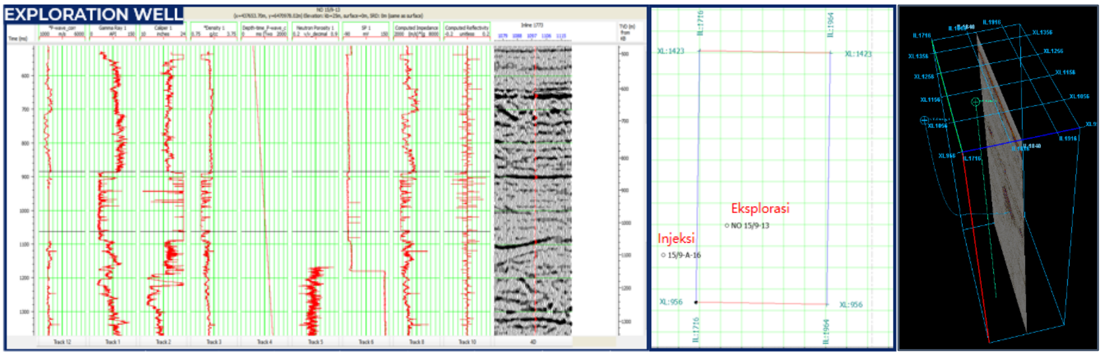

Figure 4. Exploration Data Well, Display of base map and trejectory of well location in seismic survey.

Cross-equalization

The overburden zone is the focus of research in this process, and seismic data from the overburden zone is in the 200 ms to 700 ms window, which is chosen based on seismic data analysis. This cross-equalization process compares the phase, time, amplitude, and frequency of monitor data from 200 ms to 750 ms (overburden zone) to baseline data. This process is carried out in three stages, namely phase-time shift, which aims to match the time shift and phase in the overburden zone (window 200 ms -750 ms). The shaping filter process, which aims to match the seismic frequency and amplitude from the previous phase-time shift process, comes next. Finally, there is a time-variant shift, where the monitor data movement moves randomly, not in bulk shifts to match the baseline data in all windows, the time-variant shift process is to match the monitor data with the data. baseline based on repeated acquisition and time range of processing.

Normalized root mean square (NRMS)

The repeatability value is calculated from the Normalized Root Mean Square (NRMS) Amplitude value, a low NRMS value has a high repeatability value, meaning that when NRMS is low, the monitor data and the baseline have almost the same match. Processing factors influence the size of the NRMS value.

To obtain the NRMS and repeatability values, the processing factor that can determine the match between the baseline and high monitors is to first perform a process known as cross-equalization, which matches seismic data due to differences in amplitude in the overburden zone caused by well activity or acquisition effects. by matching the phase, time shift, amplitude, and frequency of baseline and monitor seismic data, so that both data are similar to the overburden zone.

4-dimensional inversion

4-dimensional inversion is an inversion used to obtain information on changes in acoustic impedance in baseline and monitor data so that changes in acoustic impedance in both seismic data can be seen in detail. It will be useful to perform inversions while creating this initial model, where the initial model is to create a p-wave/sonic/velocity model that sees velocity information in each layer, followed by a density model that sees rock density information in each layer. The p-impedance model is obtained by multiplying the p-wave/sonic/Velocity model by the density model in order to see the distribution of acoustic impedance values in the reservoir and non-reservoir zones. Low Frequency Model is useful for adding previously missing low frequency models, and it will be added between the horizons created in both the baseline and monitor surveys, by using a lowpass filter to obtain lower frequency data from the well data (Figure 5).

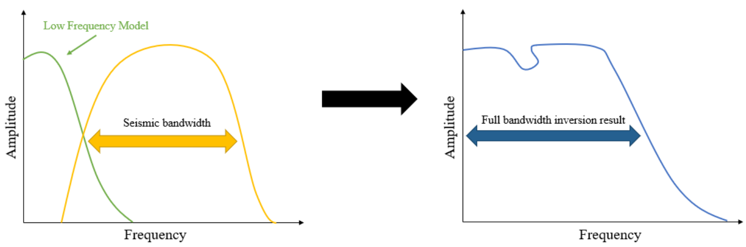

Figure 5. Schematic of adding low frequency model.

Model-based inversion, which includes deterministic inversion with the goal of minimizing errors between seismic data and synthetic data, can compare seismic data and geological models and is used iteratively to update the model to suit seismic data (Francis. 2005).

The final step in performing a 4-dimensional inversion is the inversion of seismic data that has been cross-equalization (a process that has carried out phase-time shift, shaping filter, and time-variant shift).

RESULTS AND DISCUSSION

Cross-equalization results analysis

Before analyzing the cross-equalization process (phase-time shift, shaping filter, time-variant shift), the original NRMS value in both seismic data and the amplitude spectrum form that has not been carried out in the cross-equalization process should be seen. as a starting point for the cross-equalization procedure.

The NRMS value in Figure 6 shows that the two seismic data have an average value of 0.794901, which when associated with the repeatability value in Table 1 is still classified as poor repeatability or the compatibility of the two data in the overburden zone is still very poor.

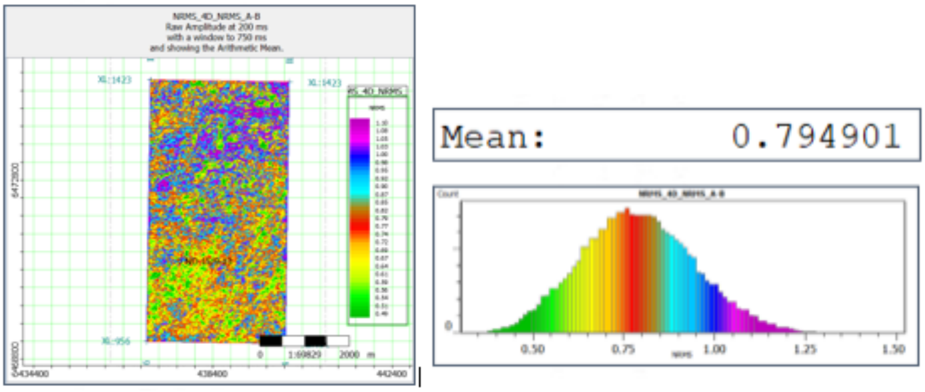

Figure 6. NRMS value on the two seismic data slices at time window 200ms – 750ms.

Phase-time shift

The first cross-equalization process, the phase-time shift, which the parameters performed with a time shift of -0.243889 and phase shift -12.5937, resulted in insignificant changes to the phase and time of the seismic data. This has a minor impact on the NRMS value, as the average NRMS value of the two original seismic data, which was originally 0.794901, has only changed to 0.788541 in this process and is still classified as poor repeatability, indicating that the two data are still very different or do not match in the overburden zone (Figure 7).

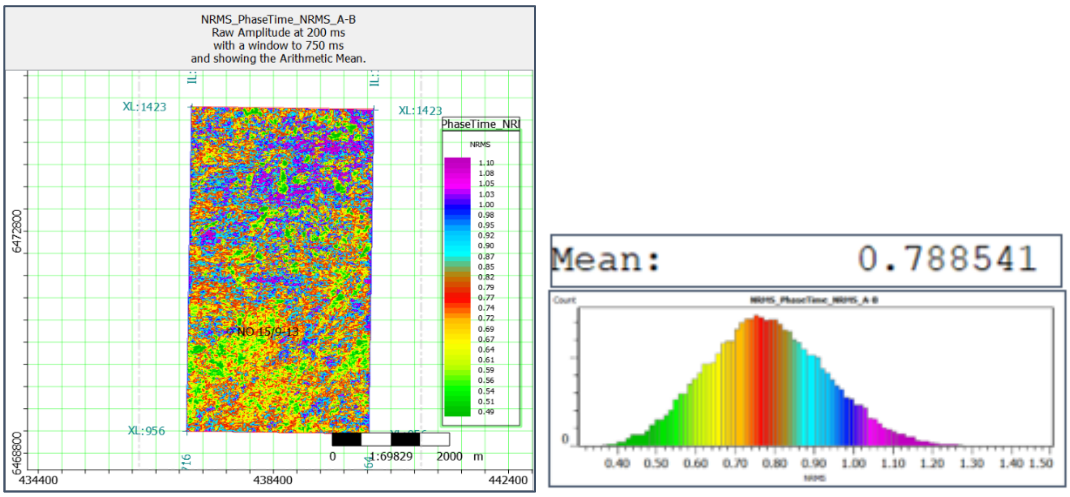

Figure 7. The NRMS value of the Slice of the phase-time shift on time window 200 ms – 750 ms.

Shaping filter

The shaping filter is the next analysis of the cross-equalization process, this process is a continuation of the previous process, namely phase-time shift. Whereas in the previous process, the results were still classified as poor repeatability or the two data did not match. The previous process aimed to match phase and time, whereas this process aimed to match frequency and amplitude. This is also comparable to the average NRMS value obtained, which changed from 0.788541 to 0.772738 in the previous process. The results are still classified as poor repeatability, but the NRMS value has decreased, indicating that this result is better than before (Figure 8).

Journal of Earth Energy Engineering
Vol. 12 No. 2s 2023: IC-UPERTAIN 2022, pp 53-66

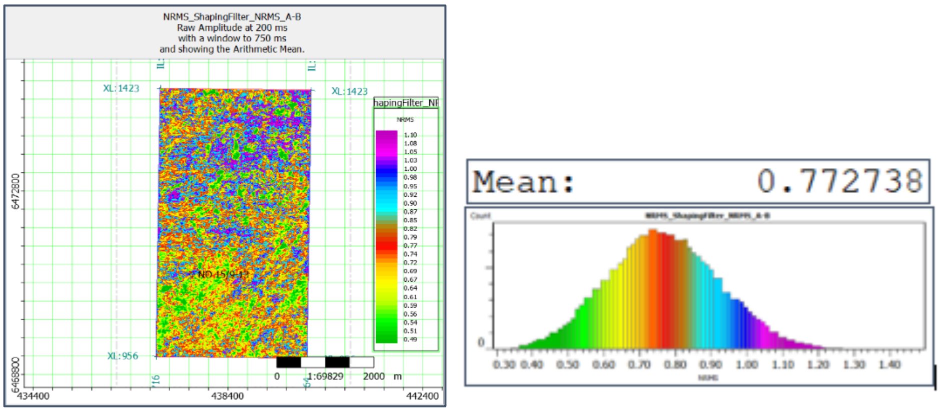

Figure 8. NRMS value from shaping filter that is sliced on time window 200 ms – 750 ms.

Time-variant shift

The analysis of the last cross-equalization process is time-variant shift, the results obtained from this process are the best after several times changing parameters. Whereas in this process the average NRMS value is 0.54639 (Figure 9) with time shift 0.0297576 and have cross correlation 0.854458 between two seismic data after this process, which value refers to Table 1 that the results are acceptable because they are classified as reasonable repeatability.

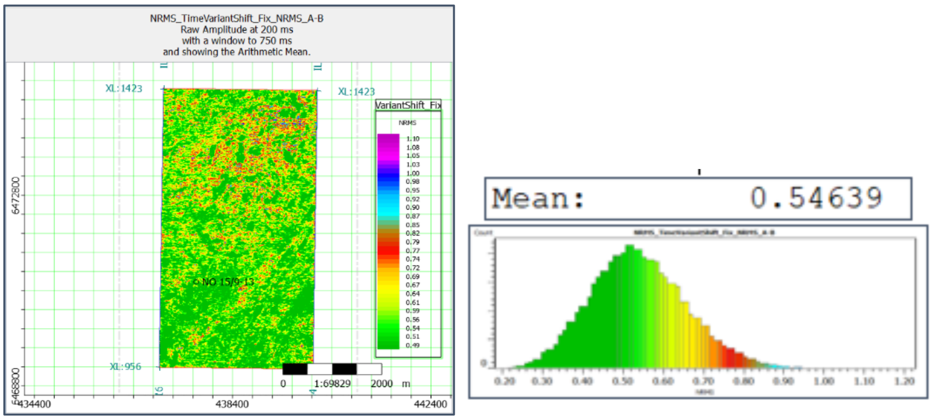

Figure 9. The NRMS value of the time-variant shift in Slice on time window 200 ms – 750 ms.

Normalized root mean square results analysis

Figure 10 shows that the NRMS value (Table 1) decreased in each cross-equalization process, in the original seismic data the two data had a very poor match with an average NRMS value of 0.794901, after the data was processed in phase-time shift and shaping filter, both seismic data only showed a slight decrease in NRMS values, namely 0.788541 and 0.772738, the data was still in poor repeatability condition in this process phase. The change in NRMS value decreased significantly by 0.54639 after applying the time-variant shift process, with the classification as reasonable repeatability. The two data sets matched with these results, but they could be improved. This result will be used in the following process, which is the 4-dimensional inversion.

$$NRMS = \frac{2\ RMS\ (a-b)}{RMS\ (a)+RMS\ (b)} \quad (1)$$

Where:
a is Monitor data
b is Baseline data

Table 1. NRMS values of the match between baseline and monitor data (Lumley, 2019)

NRMS	*Comment*
< 0.1	*Outstanding repeatability*
< 0.2	*Excellent repeatability*
0.2 – 0.4	*Very good repeatability*
0.4 – 0.6	*Reasonable repeatability*
0.6 - 0.8	*Poor repeatability*
0.8 – 1.2	*Highly non repeatability*
1.40	*Equivalent to two random data sets*
2.00	*Data sets are identical, but polarity reversed*

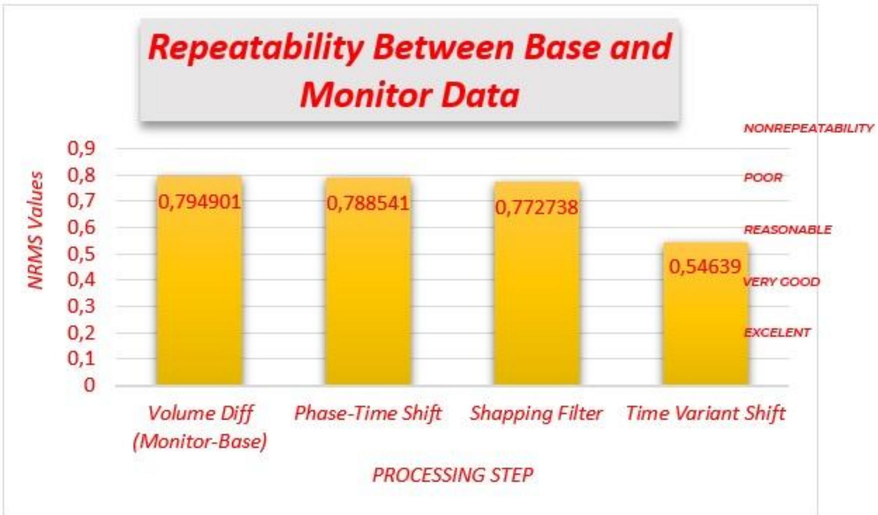

Figure 10. Baseline and monitor data repeatability values in the cross-equalization process.

Volume different after cross-equalization process

This volume of difference process examines the difference in the amplitude of seismic data in which the monitor data has an amplitude change from the baseline data with a 10-year interval, which is caused by the effects of production and CO_2 injection. In this process, to see the difference in amplitude between the two data, subtract the amplitude data across the seismic window on the monitor data from the baseline data.

The amplitude difference data on the two seismic data is shown in Figure 11. A positive different result indicates that the amplitude of the monitor data at the same time and bin is greater than the amplitude of the baseline data. Meanwhile, the negative different result indicates that the baseline data amplitude is greater than the monitor data amplitude.

Journal of Earth Energy Engineering
Vol. 12 No. 2s 2023: IC-UPERTAIN 2022, pp 53-66

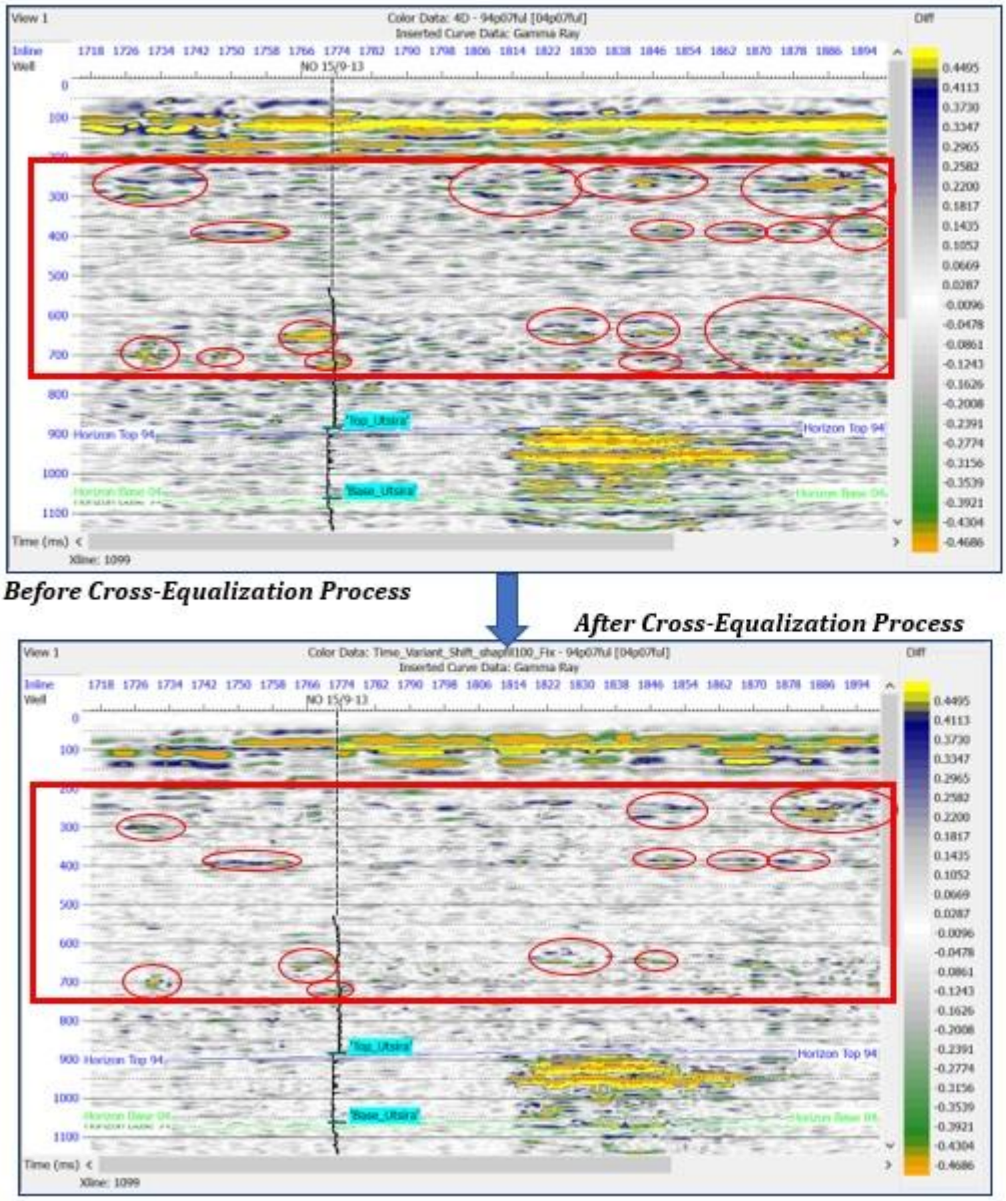

Figure 11. Volume different before cross-equalization/raw data seismic monitor - baseline (above) and volume different after cross-equalization seismic monitor - baseline (bottom).

The Volume Different on the original seismic shows that there are still many low and high diff values in the overburden zone, indicating that the differences between the two seismic data are still very different. After performing the Cross-Equalization process, the low and high diff values have been reduced, indicating that both data have seismic amplitude the same time and bin for each seismic data, indicating that the two seismic data matches. The presence of natural gas in the overburden zone is responsible for the volume differences that remain high and low after the cross-equalization process (Torus, 2022). Figure 12 depicts the change in the amplitude spectrum of the original seismic data after the cross-equalization method, with the blue curve representing the baseline seismic data and the green curve representing the seismic monitor data. The green color curve after the cross-equalization method is nearly identical to the blue color curve from the form and pattern. This also suggests that the two seismic data sets match and have nearly identical amplitude spectrum.

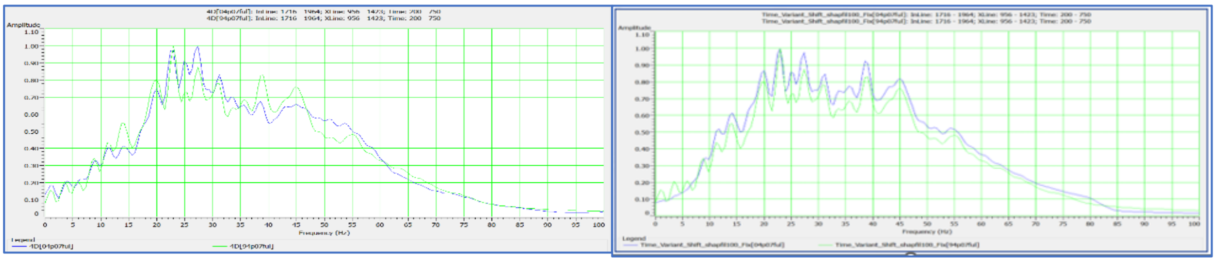

Figure 12. Amplitude spectrum of both seismic data, raw seismic data (left) and seismic data after cross-equalization (right).

Rock physics analysis

According to Arista, when CO_2 is injected, P velocity changes by 8%; in Figure 13, P velocity decreases with increasing CO_2 saturation; initially, P velocity is 1.875 km/s, but drops sharply when CO_2 saturation increases 20% to 1.7 km/s. The bulk density of rock is shown in Figure 14 as increasing CO_2 saturation causes it to become low. These changes are influenced by the lower CO_2 density than water and the addition of CO_2 saturation in the reservoir rock. Changes in the reservoir's velocity and density due to CO_2 injection will change the value of the acoustic impedance; as the velocity and density decrease, so will the acoustic impedance. Acoustic impedance decreases as CO_2 saturation increases due to CO_2 injection. The change in acoustic impedance after replacing the rock pore-filling fluid with CO_2 is 12%, as shown in Figure 15 for the different AI section.

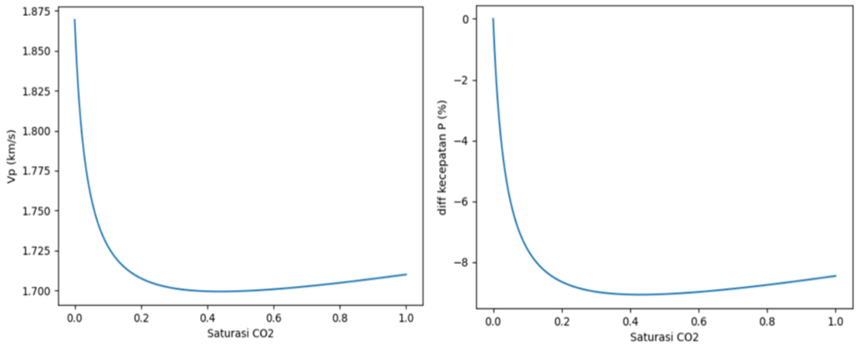

Figure 13. P velocity changes with CO_2 saturation (Arista, 2022).

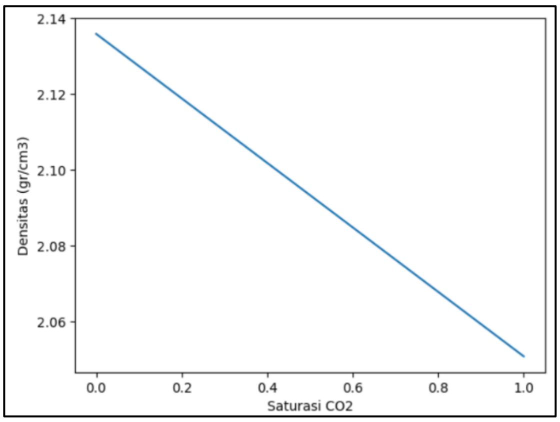

Figure 14. Bulk density changes (Arista, 2022).

Journal of Earth Energy Engineering
Vol. 12 No. 2s 2023: IC-UPERTAIN 2022, pp 53-66

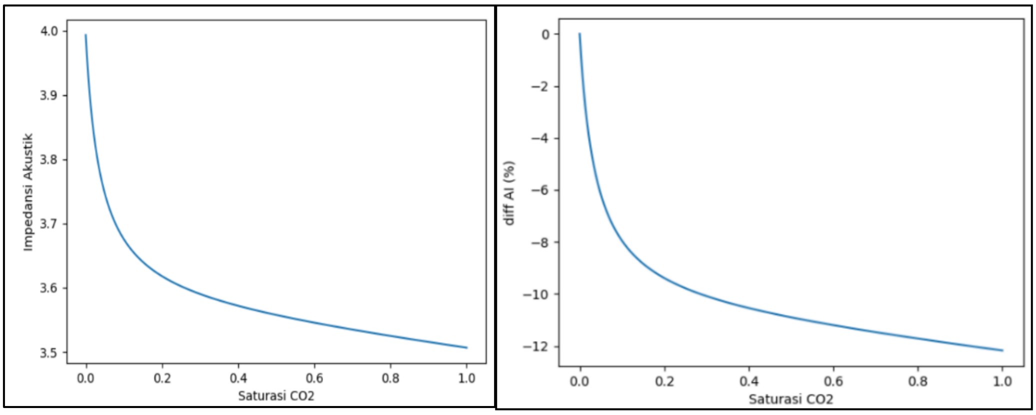

Figure 15. AI value change and percentage change in relation to CO_2 saturation (Arista, 2022).

Because CO_2 injection is carried out at the utsira reservoir depth, the decrease in density values, P wave velocity, and acoustic impedance occurs only at the utsira reservoir interval. Figure 16 depicts the changes in these values, with the black curve representing the value prior to CO_2 injection and the red curve representing the value after CO_2 injection.

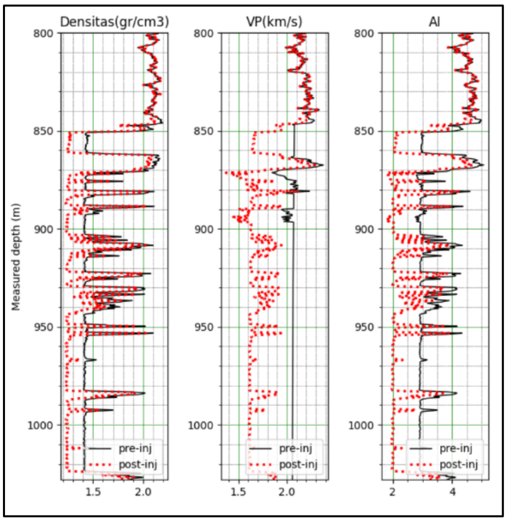

Figure 16. Changes in bulk density, P velocity, and acoustic impedance after CO_2 injection (Arista, 2022).

Inversion results analysis

Because this inversion can match the geological model below the surface, it is very suitable to be used in this CO_2 monitoring study to see the development of CO_2 injection in the utsira sandstone formation. The purpose of this inversion process is to determine the impedance value of CO_2, see how the distribution process CO_2 and ensure that CO_2 is stored safely or does not leak in the top reservoir, and see the pushdown effect in the base reservoir. So that the inversion results have a window span from the top reservoir -50 ms to the base reservoir +50 ms to see if there is a leak in the trap zone and to see the pushdown effect in the base reservoir zone.

The results of the inversion of the two seismic data are shown in Figures 17 and 18, where the impedance obtained ranges from 4876 to 2128 ((m/s)*(g/cc)). It is very clear that there is an impedance difference in the two data, namely on the monitor data the appearance of a low impedance value indicated by a thin black circle in Figure 18, the low impedance value is suspected to be CO_2 stored in the utsira sandstone formation. When CO_2 is injected, the CO_2 movement will automatically go straight to and approach the top of the reservoir and then spread laterally to cause a supercritical effect where CO_2 pushes the saline aquifer and replace it on the spot. The thick black circle in Figure 18 depicts a pushdown effect on the base reservoir caused by continuous supercritical CO_2 injection, resulting in a depressed base reservoir that will eventually experience downward compression.

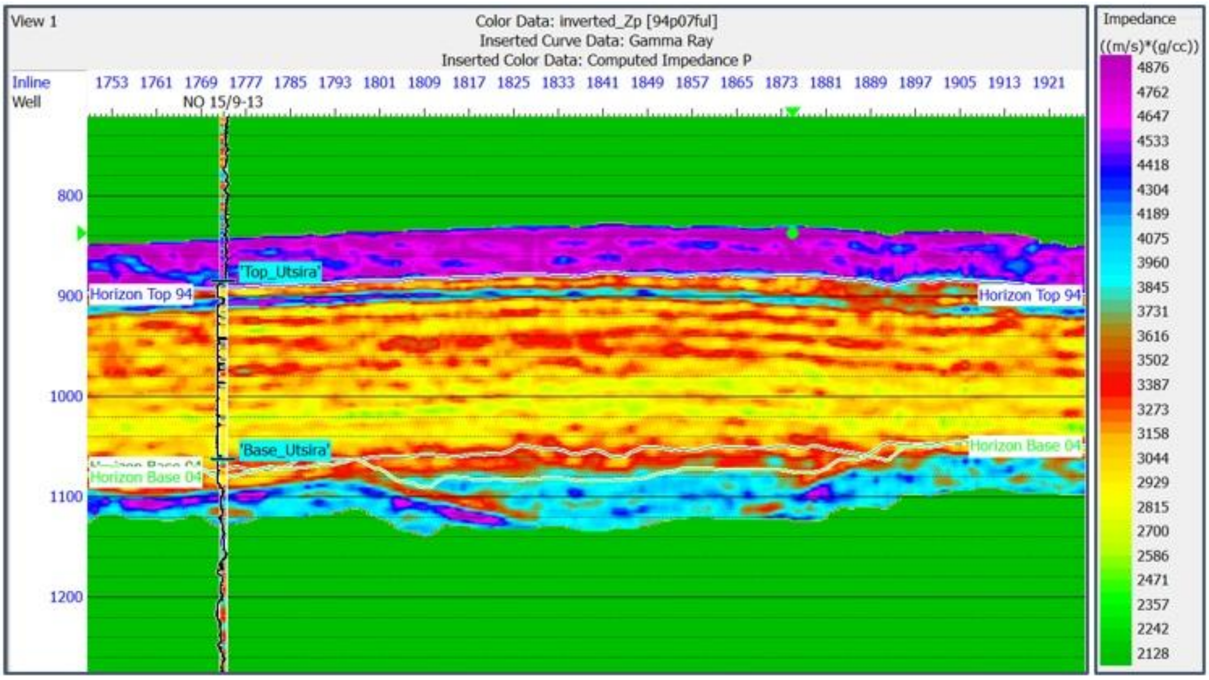

Figure 17**.** Inversion Model based Time Variant Shift Baseline data.

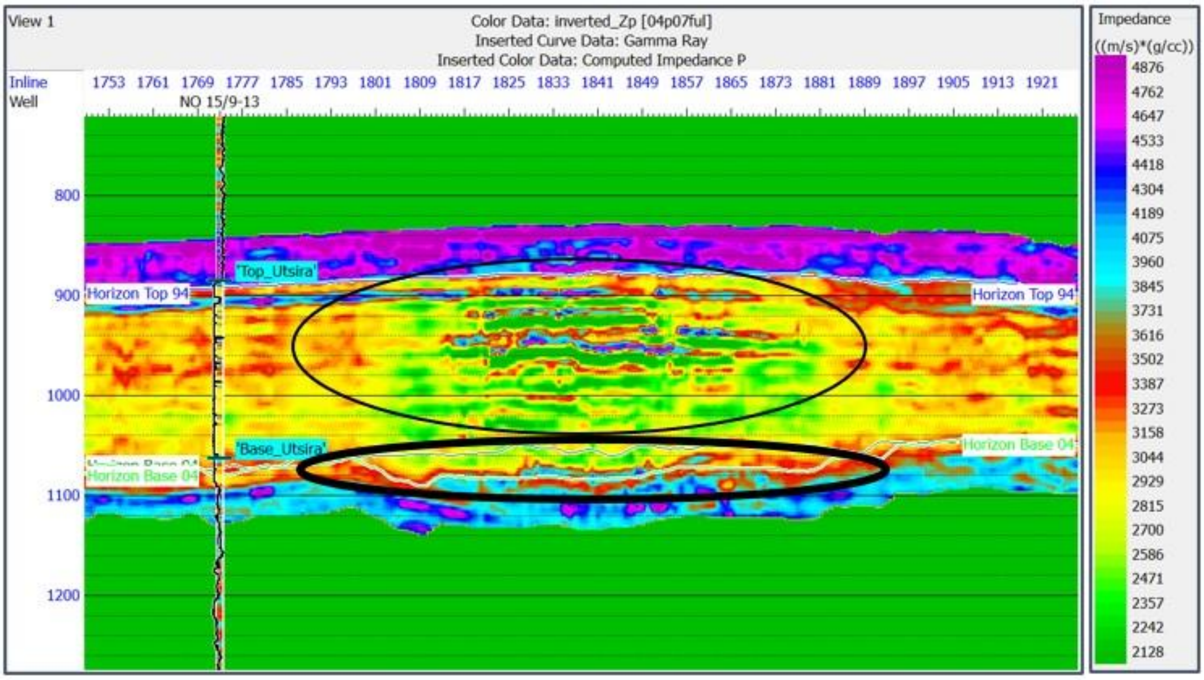

Figure 18. Inversion Model based Time Variant Shift Monitor data.

After obtaining the inversion results for the two seismic data, the difference between the inversions on the monitor data and the baseline data is calculated as ((AI monitor - AI baseline)/AI baseline) x 100 percent, in order to better understand the distribution of CO_2 impedance and the percentage of CO_2 that replaces the saline aquifer in the reservoir. Figure 19 depicts the inversion difference in two seismic data sets that has been cut in the form of a percentage and only takes a low impedance value. The percentage of CO_2 used to replace the saline aquifer in the reservoir zone ranges from 7.5% to 12.9%. As shown in Figure 20, the distribution of CO_2 has spread laterally in a northeast-southwest direction.

Figure 21 shows the impedance results between the AI monitor and AI baseline, in addition to the difference in impedance values between the two seismic data sets. It seeks to determine the cut-off value of the CO_2 impedance that replaces the saline aquifer in the reservoir zone and demonstrates that the CO_2 distribution pattern in Figure 21 and 19 is consistent.

Journal of Earth Energy Engineering
Vol. 12 No. 2s 2023: IC-UPERTAIN 2022, pp 53-66

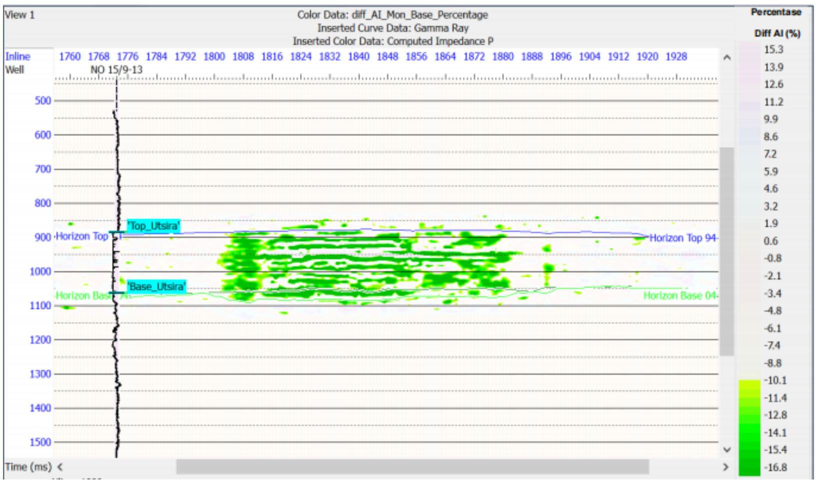

Figure 19. Results of different AI monitors and AI Baseline.

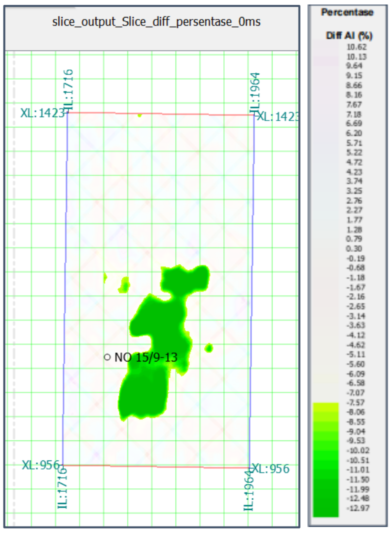

Figure 20. Slicing results of different AI monitors and AI Baseline.

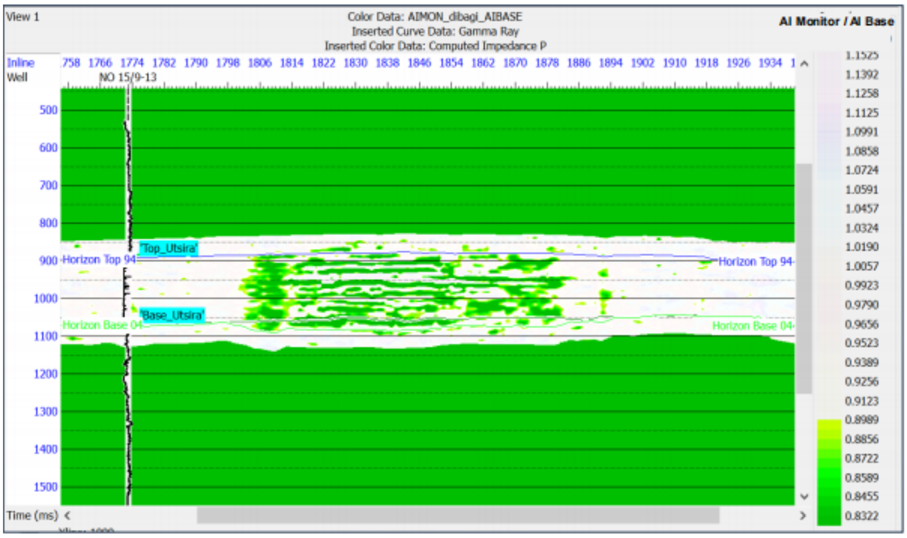

Figure 21. Results of AI monitor / AI Baseline.

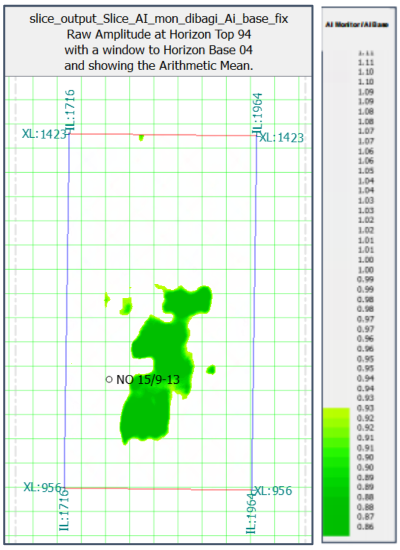

Figure 22. Results of Slicing AI monitor / AI Baseline.

Analysis of the development of CO_2 accumulation

Torus explained in 2001 that CO_2 injection in the reservoir replaces the saline aquifer, as evidenced by the results of his research inversion, which show that CO_2 injection will experience a decrease in acoustic impedance in the reservoir zone due to a decrease in velocity and density, which replaces the saline aquifer. Figure 23 shows that the spread of CO_2 has spread laterally, but it is still not too wide.

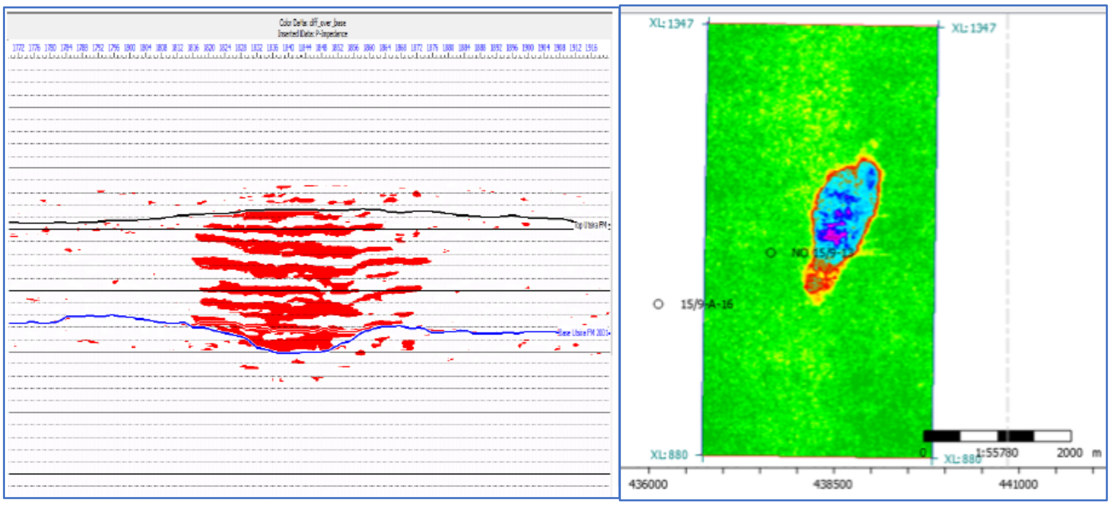

Figure 23. Distribution of CO_2 in 2001 (Torus, 2022).

When compared to the findings of this study, CO_2 was also more widely distributed laterally in 2004 than in 2001, with the direction of the spread of laterally stored CO_2 injection being northeast-southwest. Furthermore, it was confirmed in 2004 that the CO_2 in the reservoir was properly stored and did not leak (Figure 24).

Journal of Earth Energy Engineering
Vol. 12 No. 2s 2023: IC-UPERTAIN 2022, pp 53-66

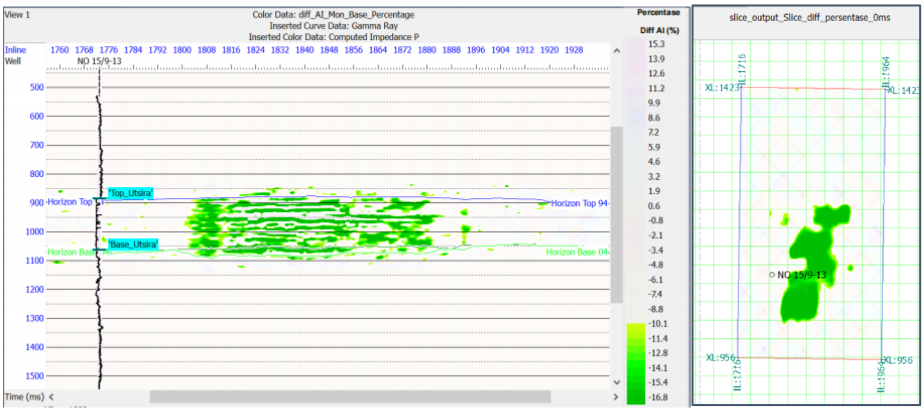

Figure 24. Distribution of CO_2 in 2004.

CONCLUSION

The matching of the two seismic data in each phase experienced a decrease in the NRMS value during the cross-equalization process, where the NRMS value in the two seismic data was initially 0.794901, which was classified as poor repeatability data, and changed to reasonable repeatability with an NRMS value of 0.54639. After implementing the cross-equalization process, both data have matched the overburden zone but need to be improved again until it reaches the maximum NRMS value.

The inversion results show that the distribution of CO_2 in the reservoir with a low impedance spread laterally in a northeast-southwest direction. The obtained inversion results also show that CO_2 is safely stored in the reservoir and does not penetrate the hood layer, as well as that the base reservoir has a pushdown effect due to continuous CO_2 injection.

Acknowledgements

The authors would like to thank Geosoftware for granting Hampson-Russell software to our department. The authors also thank equinor for providing open-source data in the form of seismic data and well data on the co2datashere.org website, which the author used for this research.

References

Arista, Y. K. (2022). *Pemodelan fisika batuan untuk injeksi CO_2 di Lapangan Sleipner, Laut Utara, Norwegia* [Rock physics modeling for CO2 injection in the Sleipner Field, North Sea, Norway] [Unpublished dissertation]. Universitas Pertamina.

Chadwick, R. A., Arts, R., & Eiken, O. (2005). *4D seismic quantification of a growing CO2 plume at Sleipner, North Sea. Petroleum Geology Conference Series*, *6*, 1385–1399. https://doi.org/10.1144/0061385

Chadwick R. A. (2010). Measurement and monitoring technologies for verification of carbon dioxide (CO2) storage in underground reservoirs. In M. M. Maroto-Valer (Ed.), *Developments and innovation in carbon capture and storage technology: Volume 2 Carbon dioxide storage and utilization* (pp. 203–239). Woodhead Publishing Ltd. https://doi.org/10.1533/9781845699581.2.203

Chadwick R. A., Williams, G., Clochard, V., Labat, K., Sturton, S., Buddensiek, M.-L., Dillen, M., Lima, A. L., Arts, R., Neele, F., & Rossi, G. (2010). Quantitative analysis of time-lapse seismic monitoring data at the Sleipner CO2 storage operation. *The Leading Edge*, *29*(2), 113–240. https://doi.org/10.1190/1.3304820

Francis, A. (2005). Limitations of deterministic and advantages of stochastic seismic inversion. *Canadian Society of Exploration Geophysicist Recorder*, *30*, 5–11.

Lumley, D. (2019). *The role of geophysics in carbon capture and storage.* In T. Davis, M. Landrø, & M. Wilson (Eds.), *Geophysics and geosequestration* (pp. 11–53). Cambridge University Press. https://doi.org/10.1017/9781316480724.003

Norwegian Petroleum Directorate. (2011). *NPD CO_2 storage atlas*. NPD. https://www.npd.no/en/facts/publications/co2-atlases/co2-atlas-for-the-Norwegian-continental-shelf/4-the-Norwegian-north-sea/4.1-geology-of-the-north-sea/

Solheim, V. M. (2021). *Seismic monitoring of CO2 sequestration – effects of saturation, pressure and temperature* [Master thesis, University of Bergen]. https://bora.uib.no/bora-xmlui/handle/11250/2763240

Torus, B. (2022). *Inversi seismik 4D untuk monitoring injeksi CO_2 pada proyek carbon capture and storage di formasi Utsira, Lapangan Sleipner, Laut Utara, Norwegia* [4D seismic inversion for monitoring CO2 injection in a carbon capture and storage project in the Utsira formation, Sleipner Field, North Sea, Norway] [Unpublished dissertation]. Universitas Pertamina.